

# Lawrence Berkeley National Laboratory

## Recent Work

### Title

A SEMICLASSICAL MULTICHANNEL BRANCHING MODEL FOR DESCRIBING STATE-SPECIFIC UNIMOLECULAR DECOMPOSITION AND OTHER DYNAMICAL PROCESSES IN POLYATOMIC MOLECULAR SYSTEMS

### Permalink

<https://escholarship.org/uc/item/3kd17182>

### Authors

Waite, B.A.  
Miller, W.H.

### Publication Date

1981-10-01



# Lawrence Berkeley Laboratory

UNIVERSITY OF CALIFORNIA

## Materials & Molecular Research Division

Submitted to the Journal of Chemical Physics

RECEIVED  
LAWRENCE  
BERKELEY LABORATORY

A SEMICLASSICAL MULTICHANNEL BRANCHING MODEL  
FOR DESCRIBING STATE-SPECIFIC UNIMOLECULAR  
DECOMPOSITION AND OTHER DYNAMICAL PROCESSES  
IN POLYATOMIC MOLECULAR SYSTEMS

FEB 22 1982

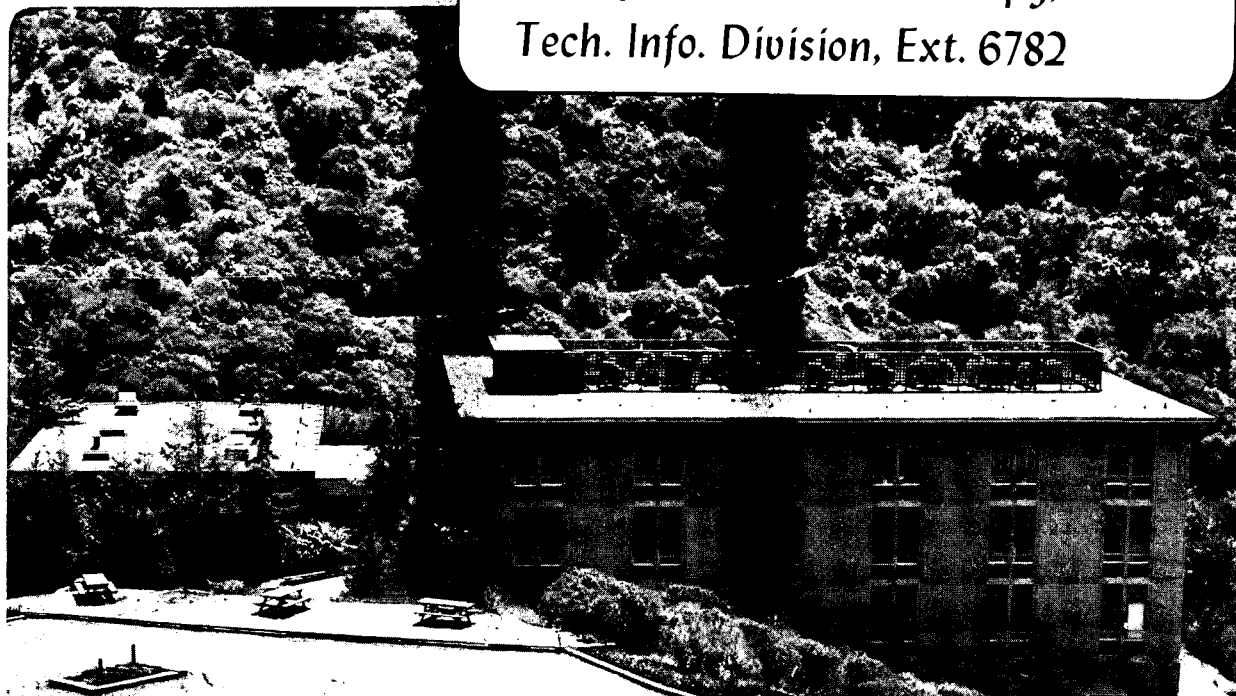
LIBRARY AND  
DOCUMENTS SECTION

Boyd A. Waite and William H. Miller

October 1981

**TWO-WEEK LOAN COPY**

*This is a Library Circulating Copy  
which may be borrowed for two weeks.  
For a personal retention copy, call  
Tech. Info. Division, Ext. 6782*



LBL-13433  
e.d.

## **DISCLAIMER**

This document was prepared as an account of work sponsored by the United States Government. While this document is believed to contain correct information, neither the United States Government nor any agency thereof, nor the Regents of the University of California, nor any of their employees, makes any warranty, express or implied, or assumes any legal responsibility for the accuracy, completeness, or usefulness of any information, apparatus, product, or process disclosed, or represents that its use would not infringe privately owned rights. Reference herein to any specific commercial product, process, or service by its trade name, trademark, manufacturer, or otherwise, does not necessarily constitute or imply its endorsement, recommendation, or favoring by the United States Government or any agency thereof, or the Regents of the University of California. The views and opinions of authors expressed herein do not necessarily state or reflect those of the United States Government or any agency thereof or the Regents of the University of California.

A Semiclassical Multichannel Branching Model for Describing State-Specific  
Unimolecular Decomposition and Other Dynamical Processes in Polyatomic  
Molecular Systems

By

Boyd A. Waite and William H. Miller

Department of Chemistry, and Materials and Molecular Research Division,  
of the Lawrence Berkeley Laboratory, University of California,  
Berkeley, California 94720

This work has been supported by the Director, Office of Energy Research,  
Office of Basic Energy Sciences, Chemical Sciences Division of the  
U.S. Department of Energy under Contract Number W-7405-ENG-48; and by  
a National Science Foundation Grant Number CHE-79-20181.

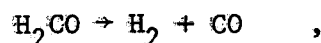
Abstract

A semiclassical multichannel branching model is developed and applied to various dynamical phenomena in polyatomic molecular systems. The model is based on the reaction path Hamiltonian of Miller, Handy and Adams [J. Chem. Phys. 72, 99 (1980)] and also utilizes the semiclassical perturbation-infinite order sudden approximation of Miller and Shi [J. Chem. Phys. 75, 2258 (1981)] for describing vibrational inelasticity along the reaction path. Specific applications of the model are made to state-specific unimolecular decomposition, energy level splitting in multidimensional double-well potentials, and to reaction probabilities along reaction paths with multiple transition states.

## I. Introduction

Recent work by us<sup>1</sup> has been concerned with the state-specific unimolecular decomposition of polyatomic molecules. The goal is to discover the relevant factors which determine whether a molecule behaves statistically in its unimolecular decay, even at the level of individual quantum states, or is mode-specific.<sup>2</sup> (By the latter we mean that different quantum states, though they have essentially the same total energy, have significantly different rates of unimolecular decay.) To this end we considered several model problems--systems consisting of two coupled oscillators, one of which could dissociate--and carried out numerically exact quantum mechanical calculations for the energies and decay rates (i.e., inverse lifetimes) of the individual quantum states (actually metastable, or resonance states) of the system. Various choices of the parameters in these model systems produced statistical or mode-specific behavior in the state-specific unimolecular decay.

Quantum mechanical calculations such as these<sup>1</sup> are no doubt the rigorously correct way to characterize state-specific unimolecular decay, but they are unfortunately not feasible for systems of more than two or three vibrational degrees of freedom (to say nothing of rotation, which we are ignoring for the present). The unimolecular decomposition of formaldehyde, for example,



is one target of our work, but it has six vibrational degrees of freedom and is thus beyond the capabilities of this rigorous approach.

One possible way to avoid these difficulties is to use classical, rather than quantum, mechanics to describe the process, i.e., to carry out a classical trajectory simulation of the unimolecular decomposition. There have indeed been many such calculations,<sup>3</sup> and in many (perhaps most?) situations there is no reason to believe that this does not describe the process correctly. In the energy region of the formaldehyde decomposition where the reaction proceeds by tunneling,<sup>4</sup> however, a classical trajectory approach is clearly inadequate.

Furthermore, there may be cases for which the unimolecular decay, though energetically possible classically, simply does not take place via classical mechanics. Hase,<sup>5</sup> for example, has seen this, i.e., quasi-periodic trajectories which have enough energy to dissociate classically but which do not. Heller<sup>6</sup> has discussed this under the term "dynamic tunneling". In the language of classical S-matrix theory<sup>7</sup> it is simply an example of a "classically forbidden" process. If this situation maintains, then classical mechanics gives zero for the rate of unimolecular decomposition, whereas in reality (i.e., quantum mechanically) the rate is non-vanishing.

Thus there are situations for which a quantum mechanical description of the unimolecular decay will be necessary, but as noted above the completely rigorous quantum mechanical approach is not feasible for more than three-atom systems. The purpose of this paper, therefore, is to describe and illustrate an approximate quantum mechanical model for determining state-specific unimolecular decay rates, one which is

capable of being applied to polyatomic molecular systems of interest and, though not rigorously correct, has a good chance of being at least semi-quantitatively accurate.

The model we have developed, which is presented in Section II, is an extension and combination of several different methodologies that one of us and colleagues have developed in recent years. First, it is a multichannel version of a semiclassical branching model that has been earlier shown<sup>7b,8</sup> to describe unimolecular decay in one-dimensional systems correctly; the multichannel aspect of it is what extends the model from one-dimension to many dimensions (i.e., degrees of freedom). At the level of implementation we have also utilized the reaction path Hamiltonian<sup>9</sup> model to characterize the polyatomic molecular system; this describes the molecular dynamics as motion along a reaction coordinate which is coupled to transverse, locally harmonic vibrational modes. Finally, we have also utilized the recently developed semiclassical perturbation-infinite order sudden (SCP-IOS) approximation<sup>10</sup> for treating vibrational inelasticity in the transverse vibrational modes as the system moves along the reaction coordinate. Applications of the model to state-specific unimolecular decay are presented in Section III, and one sees that it is able to reproduce rather well the rigorous quantum mechanical results of the two-dimensional model systems studied previously.

This semiclassical multichannel branching model is capable, however, of describing other dynamical phenomena than state-specific unimolecular decay. For example, Section IV shows how it can be used to determine energy eigenvalues of a polyatomic system, in particular



those of a double-well potential which is coupled to the other transverse vibrational modes. Section V shows that it can also be used to extend the "unified statistical" model<sup>11</sup> of chemical reaction rates to include the effects of inelasticity between the transverse vibrational modes along the reaction coordinate.

## II. The Semiclassical Multichannel Branching Model

### A. Construction of the S-matrix

Consider non-reactive scattering on a potential energy surface for which the potential energy along the reaction coordinate  $s$  is as depicted in Figure 1; the system begins at  $s = +\infty$ , moves to the left, collides, and eventually returns to  $s = +\infty$ . If there are  $F$  degrees of freedom overall, there are  $F-1$  vibrational degrees of freedom orthogonal to the reaction coordinate (which are not shown in Figure 1).

We wish to construct the S-matrix for total energy  $E$ ,

$$\underset{\approx}{S}(E) \equiv \underset{\approx}{S} \equiv \{ \underset{\approx}{S}_{\underset{\approx}{n}, \underset{\approx}{n}'} \} \quad , \quad (2.1)$$

which are the amplitudes for transitions between an initial state  $\underset{\approx}{n} \equiv (n_1, n_2, \dots, n_{F-1})$  and final state  $\underset{\approx}{n}' \equiv (n'_1, n'_2, \dots, n'_{F-1})$  of the transverse vibrational modes at  $s = +\infty$ . The idea of the branching model is to approximate this net amplitude  $\underset{\approx}{S}$  as a sum of amplitudes constructed from the different "trajectories" which can arise from tunneling through the barrier in Figure 1. Figure 2 depicts the first three such "trajectories": the first is reflected by the barrier without tunneling, the second tunnels through and makes one oscillation in the well before tunneling back out, the third tunnels through and makes two oscillations in the well before tunneling back out, and so on. The amplitude associated with the first "trajectory" is

$$S_{\approx\text{out}} \cdot (1-P)_{\approx\approx}^{1/2} \cdot S_{\approx\text{in}} \quad , \quad (2.2a)$$

that associated with the second "trajectory" is

$$S_{\approx\text{out}} \cdot P_{\approx\approx}^{1/2} \cdot S_{\approx 0} \cdot P_{\approx\approx}^{1/2} \cdot S_{\approx\text{in}} \quad , \quad (2.2b)$$

and that with the third "trajectory" is

$$(-1) S_{\approx\text{out}} \cdot P_{\approx\approx}^{1/2} \cdot S_{\approx 0} \cdot (1-P)_{\approx\approx}^{1/2} \cdot S_{\approx 0} \cdot P_{\approx\approx}^{1/2} \cdot S_{\approx\text{in}} \quad , \quad (2.2c)$$

and so on. In these expressions  $S_{\approx\text{in}}$  is the S-matrix (i.e., matrix of transition amplitudes) associated with the incoming motion from  $s = +\infty$  to the outer turning point  $s = s_3$  (see Figure 2);  $S_{\approx 0}$  is the S-matrix for motion in the interior well from  $s = s_2$  to  $s_1$  and back to  $s_2$ ; and  $S_{\approx\text{out}}$  is the S-matrix for the outgoing motion from  $s = s_3$  back to  $+\infty$ .  $P$  is the matrix of tunneling probabilities. Note that  $S_{\approx\text{in}}$  and  $S_{\approx\text{out}}$  are in general rectangular matrices since there are in general a different number of transverse vibrational states that are energetically open at  $s = s_3$  and  $s = +\infty$ ; thus in the matrix element  $S_{\approx\approx}^{(\text{in})}$ , for example,  $\approx'$  refers to transverse vibrational states at  $s = +\infty$ , and  $\approx$  to those at  $s = s_3$ , while for  $S_{\approx\approx}^{(\text{out})}$  the identifications are reversed. (By symmetry, in fact,  $S_{\approx\text{out}}$  is the transpose of  $S_{\approx\text{in}}$ .)  $S_{\approx 0}$  is a square matrix, the indices of which refer to the transverse vibrational states at  $s = s_2$ . It is clear that the physical meaning of  $S_{\approx\text{in}}$  and  $S_{\approx\text{out}}$  is that they describe vibrational inelasticity in the region outside the barrier (i.e., entrance/exit channel effects), whereas  $S_{\approx 0}$ , the S-matrix per oscillation in the well, describes vibrational inelasticity in the region of the potential well. Although it is not necessary,

we assume for simplicity of presentation that  $\tilde{P}$  is a square matrix (i.e., the same number of vibrational states are open at  $s = s_2$  and  $s_3$ ), and furthermore in applications below it will even be approximated as diagonal. All the matrices are functions of the total energy  $E$ ; i.e.,  $S_{\tilde{in}} = S_{\tilde{in}}(E)$ , etc.

The net amplitude  $S$  is obtained by adding the amplitudes for all "trajectories" of the type described above,

$$S = S_{\tilde{out}} \cdot (1-P)^{1/2} \cdot S_{\tilde{in}} + \sum_{k=0}^{\infty} (-1)^k S_{\tilde{out}} \cdot P^{1/2} \cdot S_{\tilde{0}} \cdot [(1-P)^{1/2} \cdot S_{\tilde{0}}]^k \cdot P^{1/2} \cdot S_{\tilde{in}} \quad (2.3)$$

of which Eq. (2.2) gives the first three. The general  $k^{\text{th}}$  term in Eq. (2.3) has the direct mechanistic interpretation by simply reading the various factors from right to left: the system evolves from  $s = +\infty$  to  $s_3$  ( $S_{\tilde{in}}$ ), tunnels through the barrier ( $P^{1/2}$ ), oscillates in the well  $(k+1)$  times, not tunneling out each time it is reflected at  $s_2$  ( $S_{\tilde{0}} \cdot [(1-P)^{1/2} \cdot S_{\tilde{0}}]^k$ ), tunnels out through the barrier ( $P^{1/2}$ ), and finally moves from  $s_3$  back out to  $s = +\infty$  ( $S_{\tilde{out}}$ ). The factor  $(-1)^k$  enters because of the extra reflections involved in the  $k^{\text{th}}$  "trajectory". The geometric series in Eq. (2.3) is easily summed to give

$$S = S_{\tilde{out}} \cdot (1-P)^{1/2} \cdot S_{\tilde{in}} + S_{\tilde{out}} \cdot P^{1/2} \cdot S_{\tilde{0}} \cdot [1 + (1-P)^{1/2} \cdot S_{\tilde{0}}]^{-1} \cdot P^{1/2} \cdot S_{\tilde{in}} \quad (2.4)$$

Equation (2.4) is the general result for the S-matrix given by this semiclassical multichannel branching model. The semiclassical aspect of the branching model is that we have used it to construct a probability amplitude; in other instances<sup>11</sup> we have used similar branching models to construct probabilities, and within the present nomenclature we would refer to these as classical branching models (see also Section V). The multichannel aspect of the present treatment is that the quantities  $S_{\approx 0}$ ,  $P$ ,  $S_{\approx in}$  and  $S_{\approx out}$  are matrices in the transverse vibrational state quantum numbers, and as such it is necessary to maintain the correct order of the matrix products in Eqs. (2.3) and (2.4). The matrix products, which involve sums over intermediate transverse vibrational states, are a manifestation of the quantum principle<sup>12</sup> that one sums over all intermediate states that are not observed.

#### B. Complex Eigenvalues

Rather than considering a collision process as in the previous section, we now consider unimolecular decay of the collision complex, i.e., the metastable state, that is prepared in some manner that need not concern us here. The individual metastable states are characterized by complex energy eigenvalues,  $E_r - i\Gamma/2$ , the real part of which is the energy  $E_r$  of the state and the imaginary part of which determines its "width"  $\Gamma$ ; the lifetime of the state is  $\hbar/\Gamma$ , i.e., its unimolecular decay rate is  $\Gamma/\hbar$ .

The complex eigenvalues of the metastable system are defined<sup>13</sup> rigorously as the poles of the S-matrix  $S_{\approx}(E)$ , so we now use the S-matrix given by the branching model, Eq. (2.4), to determine these poles. It is clear that poles in  $S_{\approx}(E)$  occur at values of  $E$  for which the inverse

matrix in Eq. (2.4) is singular, i.e., values of E for which

$$\det \left| 1 + \left[ \frac{1-P(E)}{S_0(E)} \right]^{1/2} \right| = 0 \quad , \quad (2.5)$$

where we have emphasized that P and  $S_0$  are functions of E.

Equation (2.5) is the desired equation for determining the complex eigenvalues, i.e., the state-specific energies and lifetimes, of the metastable system. As one would intuitively expect, the equation involves only the "interior" S-matrix  $S_0$  and the tunneling probabilities, and not the "exterior" S-matrices  $S_{in}$  and  $S_{out}$ .

It is useful to check the form taken by Eq. (2.5) in several limiting cases. First, for a one-dimensional system P and  $S_0$  become 1 x 1 matrices, i.e., simple numbers, and the WKB approximation for them is

$$S_0(E) = e^{2i\phi(E)} \quad (2.6a)$$

$$P(E) = e^{-2\theta} / (1 + e^{-2\theta}) \quad , \quad (2.6b)$$

where  $\phi(E)$  is the WKB phase integral across the well and  $\theta(E)$  the usual barrier penetration integral. Eq. (2.5) then reads

$$1 + e^{2i\phi / (1 + e^{-2\theta})^{1/2}} = 0 \quad ,$$

which is equivalent to

$$\phi(E) = \left(n + \frac{1}{2}\right)\pi - \frac{1}{4} \ln(1 + e^{-2\theta}) \quad ,$$

and as has been shown before,<sup>7b</sup> for  $e^{-2\theta} \ll 1$ , this gives the usual WKB eigenvalue equation for the real part of the complex eigenvalue,

$$\phi(E_r) = (n + \frac{1}{2})\pi \quad , \quad n = 0, 1, 2, \dots \quad , \quad (2.7a)$$

with the width  $\Gamma$  given by

$$\Gamma = \left( \frac{dE_r}{dn} / 2\pi \right) e^{-2\theta} \quad . \quad (2.7b)$$

Equation (2.7) is the well-known semiclassical (i.e., WKB) result for the one-dimensional case.<sup>14</sup>

It is useful also to check the multichannel aspect of Eq. (2.5) by some simple analytic test, and one way to do so is to consider the limit in which tunneling is "turned off"; i.e., one sets  $P \approx 0$ , whereby Eq. (2.5) becomes

$$\det \left| \underset{\approx}{1} + \underset{\approx}{S}_0(E) \right| = 0 \quad . \quad (2.8)$$

In this limit the system is no longer metastable, but a truly bound molecular system with real energy levels corresponding to bound motion in the interior well coupled to the transverse vibrational modes. It is still difficult to draw any intuitive conclusions from Eq. (2.8), but in Appendix A it is shown that in the perturbative limit, i.e., that  $\underset{\approx}{S}_0$  is almost diagonal, the energy levels given by Eq. (2.8) do indeed correspond to the usual quantum mechanical perturbative expression for real energy eigenvalues.

Finally, although the derivation of Eq. (2.5) has referred to the situation in Figure 1, where the effective potential has a barrier, this

actually need not be the case. Appendix B shows that Eq. (2.5) is also capable of describing Feshbach resonances,<sup>15</sup> for which the effective potential typically has an attractive well but no barrier (as, e.g., a Morse potential). In this case metastability arises because of excitation in the region of the potential well of transverse vibrational states that are energetically forbidden in the asymptotic ( $s \rightarrow \infty$ ) region. Appendix B shows how Eq. (2.5) reproduces (with appropriate approximations) the usual Feshbach golden rule-like expression for the width of metastable states for this case.



### C. Dynamical Approximations

As discussed in the Introduction, the principle aim of the present paper is to provide an approach that can be applied to real molecular systems. To utilize Eq. (2.5) for determining the state-specific unimolecular decay rates one thus needs a relatively simple method for constructing  $S_{\approx 0}$ , the S-matrix per oscillation in the well, and  $P_{\approx}$ , the tunneling probabilities. Although any number of approaches might be used to do this, a particularly attractive one is the semiclassical perturbation-infinite order sudden approximation (SCP-IOS) discussed recently by Miller and Shi.<sup>10</sup>

The SCP-IOS approximation makes use of the reaction path Hamiltonian of Miller, Handy and Adams<sup>9</sup> for modeling the molecular system; if  $(s, p_s)$  are the mass-weighted reaction coordinate and its conjugate momentum and  $(\underline{n}, \underline{q}) \equiv (n_k, q_k)$ ,  $k = 1, \dots, F-1$ , are the action-angle variables for the transverse vibrational modes, then the classical Hamiltonian

has the form

$$H(p_s, s, \underline{n}, \underline{q}) = \frac{\frac{1}{2} [p_s - \sum_{k,k'=1}^{F-1} B_{k,k'}(s) \sqrt{(2n_k+1)(2n_{k'}+1)} \sqrt{\frac{\omega_{k'}(s)}{\omega_k(s)}} \sin q_k \cos q_{k'}]^2}{[1 + \sum_{k=1}^{F-1} B_{k,F}(s) \sqrt{\frac{2n_k+1}{\omega_k(s)}} \sin q_k]^2} + V_0(s) + \sum_{k=1}^{F-1} (n_k + \frac{1}{2}) \omega_k(s) \quad (2.9)$$

where  $V_0(s)$  is the potential energy along the reaction path,  $\{\omega_k(s)\}$  are the local harmonic frequencies of the transverse vibrational modes along the reaction path, and the matrix elements  $\{B_{k,k'}(s)\}$  couple the transverse vibrational modes to each other and to the reaction coordinate (labeled as modes  $k=F$ ). More discussion of this Hamiltonian, and how it can be constructed from ab initio quantum chemical calculations,

and the nature of the coupling elements is given in earlier papers.<sup>9,11,16,17</sup>

Since the action variables  $\{n_k\}$  are the classical counterpart to vibrational quantum numbers, this Hamiltonian provides a convenient framework for implementing the branching model developed above.

Construction of the interior S-matrix  $S_{\approx 0}(E)$  within the SCP-IOS approximation is a relatively simple adaptation of the work of Miller and Shi.<sup>10</sup> With  $\hbar=1$  everywhere the expression is

$$S_{\tilde{n}, \tilde{n}'}(E) = \frac{e^{i\phi_0}}{(2\pi)^{F-1}} \int_0^{2\pi} dq \exp[-i\Delta\tilde{n} \cdot \tilde{q} + i\Delta\phi(\tilde{q})] \quad , \quad (2.10)$$

where  $\Delta\tilde{n} = \tilde{n}' - \tilde{n}$  and

$$\phi_0 = \phi_0(\tilde{n}, E) = 2 \int_{s_1}^{s_2} ds \sqrt{2[E - V_a(s)]} \quad (2.11a)$$

$$\begin{aligned} \Delta\phi(\tilde{q}, \tilde{n}, E) = & \sum_{k=1}^{F-1} 2 \sin q_k \int_{s_1}^{s_2} ds \sqrt{2[E - V_a(s)]} B_{kF}(s) \sqrt{\frac{2n_k+1}{\omega_k(s)}} \cos[\delta_k(s)] \\ & + \sum_{k, k'=1}^{F-1} [\cos(q_k - q_{k'}) \int_{s_1}^{s_2} ds B_{kk'}(s) \sqrt{(2n_k+1)(2n_{k'}+1)} \sqrt{\frac{\omega_{k'}}{\omega_k}} \sin(\delta_k - \delta_{k'}) \\ & + \cos(q_k + q_{k'}) \int_{s_1}^{s_2} ds B_{kk'}(s) \sqrt{(2n_k+1)(2n_{k'}+1)} \sqrt{\frac{\omega_{k'}}{\omega_k}} \sin(\delta_k + \delta_{k'})] \quad . \end{aligned} \quad (2.11b)$$

with

$$\delta_k(s) = \int_{s_1}^s ds' \frac{\omega_k(s')}{\sqrt{2[E - V_a(s')]} } \quad ; \quad (2.11c)$$

and finally, in Eq. (2.11)  $\tilde{n}$  is replaced by  $\frac{1}{2}(\tilde{n} + \tilde{n}')$ , and  $V_a(s)$  is the vibrationally adiabatic potential

$$V_a(s) = V_0(s) + \sum_{k=1}^{F-1} \left( n_k + \frac{1}{2} \right) \omega_k(s) \quad . \quad (2.11d)$$

One recognizes the zero<sup>th</sup> order phase of the S-matrix,  $\phi_0$ , as the vibrationally adiabatic WKB phase integral back and forth across the well; the phase  $\Delta\phi(q)$  arises because of couplings between the various modes and thus gives rise to a non-diagonal S-matrix, i.e., to vibrational inelasticity.

One practical note concerns the unitarity of the S-matrix  $S_{\approx 0}(E)$ . Since it is a square matrix of probability amplitudes, it is clearly a unitary matrix (i.e.,  $S_{\approx}^{\dagger} \cdot S_{\approx} = S_{\approx} \cdot S_{\approx}^{\dagger} = 1$ ). The approximation to it given by Eq. (2.10) et seq. however, will not be exactly unitary, and for the applications in the next section this would cause major errors. (Also, the roots of Eq. (2.8), i.e., the real eigenvalues of a bound system, will not be real if  $S_{\approx 0}$  is not unitary!) It is thus important to unitarize any approximate  $S_{\approx 0}$  by some means. One way to do this is via an R-matrix procedure. Thus an S-matrix  $S_{\approx}$  and R-matrix  $R_{\approx}$  are related by

$$S_{\approx} = (1 - iR_{\approx}) \cdot (1 + iR_{\approx})^{-1} \quad , \quad (2.12a)$$

or inversely

$$R_{\approx} = -i(1 - S_{\approx}) \cdot (1 + S_{\approx})^{-1} \quad . \quad (2.12b)$$

If  $\tilde{S}$  is unitary then  $\tilde{R}$  is hermitian, and vice-versa. Thus if  $\tilde{S}$  is not unitary, then  $\tilde{R}$  given by Eq. (2.12b) will not be hermitian. One can make  $\tilde{R}$  hermitian, however, by simply taking its hermitian part,

$$\tilde{R}_H = \frac{1}{2}(\tilde{R} + \tilde{R}^\dagger) \quad . \quad (2.13)$$

Thus one prescription for unitarizing an approximate S-matrix is to use Eq. (2.12b) to construct the corresponding approximate R-matrix and then "hermitizing" this approximate R-matrix via Eq. (2.13). When  $\tilde{R}_H$  is then put back into Eq. (2.12a) in place of  $\tilde{R}$ , a unitary S-matrix results. The result of this prescription is that the unitarized S-matrix,  $\tilde{S}_U$ , is given in terms of the approximate S-matrix by

$$\tilde{S}_U = [\tilde{S} \cdot (1 + \tilde{S})^{-1} + \tilde{S} \cdot (1 + \tilde{S})^{-1}] \cdot [(1 + \tilde{S})^{-1} + (1 + \tilde{S})^{-1}]^{-1} \quad (2.14)$$

where

$$\tilde{S} = (\tilde{S}^\dagger)^{-1} \quad .$$

This prescription for unitarizing an approximate S-matrix is, of course, not unique. If the approximate S-matrix is too far from unitarity, however, so that the particular unitarization scheme matters, then one has less confidence in the overall model for such a case.

Finally, the tunneling probabilities  $\tilde{P}$  can also be obtained within the SCP-IOS approximation.<sup>10,17</sup> For the applications discussed in the next section the coupling elements  $\{B_{k,k'}\}$  have very little effect on the tunneling probabilities and were thus neglected. In this limit the SCP-IOS approximation becomes the vibrationally adiabatic approximation<sup>18</sup> and the matrix  $\tilde{P}$  is diagonal,

$$P_{\tilde{n},\tilde{n}'} = \delta_{\tilde{n},\tilde{n}'} e^{-2\theta} \quad , \quad (2.15)$$

where  $\theta$  is the vibrationally adiabatic barrier penetration integral,

$$\theta \equiv \theta(\tilde{n}, E) = \int_{s_2}^{s_3} ds \sqrt{2[V_a(s) - E]} \quad . \quad (2.16)$$

Equation (2.15) is valid only for small tunneling probabilities, the more generally valid expression being

$$P_{\tilde{n},\tilde{n}'} = \delta_{\tilde{n},\tilde{n}'} (1 + e^{2\theta})^{-1} \quad . \quad (2.17)$$

Equation (2.17) is meaningful even for relative energies above the barrier, in which case  $\theta(\tilde{n}, E)$ , the analytic continuation (in  $E$ ) of Eq. (2.16), is negative.

### III. Mode-Specific Unimolecular Decomposition

The first application we consider of the multichannel semiclassical branching model is to the situation discussed in Section II; i.e., we use Eq. (2.5) to determine the energies and lifetimes of a metastable system. The example chosen is one of the two-oscillator models for which we have earlier<sup>1b</sup> carried out rigorous quantum mechanical calculations. The potential function is

$$V(x,y) = \frac{1}{2}(x^2 + y^2) - \frac{1}{3}(x^3 + xy^2) \quad , \quad (3.1)$$

which is a one-barrier Henon-Heiles-like potential.

For this example the reaction path is straight (the x-axis), and the reaction path Hamiltonian thus takes the relatively simple form

$$\begin{aligned} H(p_s, s, n, q) = & \frac{1}{2} \left[ p_s + \frac{\omega'(s)}{2\omega(s)} \left( n + \frac{1}{2} \right) \sin(2q) \right]^2 \\ & + V_0(s) + \left( n + \frac{1}{2} \right) \omega(s) \end{aligned} \quad (3.2a)$$

where

$$V_0(s) = \frac{1}{2} s^2 - \frac{1}{3} s^3 \quad (3.2b)$$

$$\omega(s) = \sqrt{1 - \frac{2}{3} s} \quad . \quad (3.2c)$$

Since the complete potential function in Eq. (3.1) is quadratic in the transverse degree of freedom (i.e., in y), the reaction path Hamiltonian is actually the exact Hamiltonian for this example.

The interior S-matrix  $\{S_{n,n'}\}$  and tunneling probabilities  $P_n$

were constructed as in Section IIc. Figures 3 and 4 show the results given by the present model, i.e., Eq. (2.5), and our earlier<sup>1b</sup> rigorous quantum mechanical values, respectively. As discussed before, this example shows quite pronounced mode-specificity--i.e., the unimolecular decay rate is not at all a monotonic function of the total energy--and most significant for present considerations, one sees that the multichannel semiclassical branching model reproduces the correct results quite well. This is true even for metastable states with energies above the saddle point ( $V_{sp} = \frac{1}{6}$ ), for which the analytically continued barrier penetrations integrals discussed in Section IIc were required. This test of the overall model, including the SCP-IOS approximations for  $S_{\approx 0}$  and  $P_{\approx}$ , is thus quite encouraging.

IV. Energy Levels in a Multidimensional Double-Well Potential

As noted in the Introduction, the multichannel branching model can be used to describe other phenomena than the energies and lifetimes of metastable systems. Here we show how it describes the energy levels of a multidimensional double well potential.

Consider first inelastic scattering on a potential surface for which the potential along the reaction coordinate is as sketched in Figure 5; here again there are (F-1) transverse vibrational modes (in the spirit of the reaction path Hamiltonian) that are not depicted. We want to construct the S-matrix for this scattering system, as was done in Section II, but now there are two interior wells, separated by a barrier. The analysis of Section II can be generalized to treat the present case (or for that matter, any number of wells and barriers) by an inductive argument similar to that used earlier<sup>11</sup> to generalize a classical branching model to treat multiple wells and barriers. Thus one considers the entire region of well a, barrier 1, and well b as the "inside" region that is separated from the "outside" region by barrier 2 (see Figure 5). If  $S_{\approx 0}$  is the S-matrix that characterizes this complete "inside" region (wells a and b and barrier 1), then Eq. (2.4) applies as before to give the S-matrix as

$$S_{\approx}(E) = S_{\approx out} \cdot (1-P_{\approx 2})^{1/2} \cdot S_{\approx in} + S_{\approx out} \cdot P_{\approx 2}^{1/2} \cdot S_{\approx 0} \cdot [1+(1-P_{\approx 2})^{1/2} \cdot S_{\approx 0}]^{-1} \cdot P_{\approx 2}^{1/2} \cdot S_{\approx in}, \quad (4.1)$$

where  $S_{\approx in}$  and  $S_{\approx out}$  are the incoming and outgoing S-matrices for the "outside" region in Figure 5 and  $P_{\approx 2}$  the matrix of tunneling probabilities for barrier 2. To determine the S-matrix  $S_{\approx 0}$  in Eq. (4.1),



i.e., the S-matrix for wells a and b, separated by barrier 1, one recognizes that this complex "inside" region is equivalent to the scattering system in Figure 1 if one identifies the external scattering region of Figure 1 with the region of well b in Figure 5. Thus  $S_{\approx 0}$  in Eq. (4.1) is itself given by Eq. (2.4),

$$S_{\approx 0} = S_{\approx b, \text{out}} \cdot (1-P_{\approx 1})^{1/2} \cdot S_{\approx b, \text{in}} + S_{\approx b, \text{out}} \cdot (P_{\approx 1})^{1/2} \cdot S_{\approx a} \cdot [1 + (1-P_{\approx 1})^{1/2} \cdot S_{\approx a}]^{-1} \cdot P_{\approx 1}^{1/2} \cdot S_{\approx b, \text{in}}, \quad (4.2)$$

where  $S_{\approx a}$  is the S-matrix for motion back and forth across well a ( $s_1 \rightarrow s_2 \rightarrow s_1$ ),  $S_{\approx b, \text{in}}$  is the S-matrix for inward motion across well b ( $s_4 \rightarrow s_3$ ),  $S_{\approx b, \text{out}}$  the S-matrix for outward motion across well b ( $s_3 \rightarrow s_4$ ), and  $P_{\approx 1}$  the (square) matrix of tunneling probabilities for barrier 1. The final expression for the S-matrix for the present system is obtained by inserting Eq. (4.2) for  $S_{\approx 0}$  into Eq. (4.1). It is clear how one can extend this procedure inductively to generate the S-matrix for the case of an arbitrary number of wells and barriers.

For the present application, though, we are interested in energy levels, so we "switch off" tunneling through barrier 2, i.e., we set  $P_{\approx 2} = 0$ , and look for poles of the S-matrix  $S(E)$ . With  $P_{\approx 2} = 0$ , Eq. (4.1) shows that the poles occur at values of  $E$  for which

$$\det |1 + S_{\approx 0}(E)| = 0, \quad (4.3)$$

and with  $S_{\approx 0}$  given by Eq. (4.2) this becomes

$$\det \left| 1 + S_{\approx b, \text{out}} \cdot (1 - P_{\approx 1})^{1/2} \cdot S_{\approx b, \text{in}} + S_{\approx b, \text{out}} \cdot P_{\approx 1}^{1/2} \cdot S_{\approx a} \cdot [1 + (1 - P_{\approx 1})^{1/2} \cdot S_{\approx a}]^{-1} \cdot P_{\approx 1}^{1/2} \cdot S_{\approx b, \text{in}} \right| = 0 \quad (4.4)$$

Eq. (4.4) can be put in a more useful form by multiplying it from the left by  $\det |S_{\approx b, \text{in}}|$  and from the right by  $\det |S_{\approx b, \text{out}}|$  (recall that  $\det |A| \cdot \det |B| \cdot \det |C| = \det |A \cdot B \cdot C|$ ), recognizing that  $S_{\approx b}$ , the S-matrix per oscillation in well b ( $s_3 \rightarrow s_4 \rightarrow s_3$ ), is given by

$$S_{\approx b} = S_{\approx b, \text{in}} \cdot S_{\approx b, \text{out}} \quad ; \quad (4.5)$$

with this Eq. (4.4) becomes

$$\det \left| S_{\approx b} + S_{\approx b} \cdot (1 - P_{\approx 1})^{1/2} \cdot S_{\approx b} + S_{\approx b} \cdot P_{\approx 1}^{1/2} \cdot S_{\approx a} \cdot [1 + (1 - P_{\approx 1})^{1/2} \cdot S_{\approx a}]^{-1} \cdot P_{\approx 1}^{1/2} \cdot S_{\approx b} \right| = 0 \quad (4.6)$$

Note here that the indices of  $S_{\approx a}$  refer to transverse vibrational states at  $s_2$  and those of  $S_{\approx b}$  to transverse vibrational states at  $s_3$ , and since  $P_{\approx 1}$  is assumed to be vibrationally adiabatic, all the matrices in Eq. (4.6)-- $S_{\approx a}$ ,  $S_{\approx b}$ , and  $P_{\approx 1}$ --are thus square matrices of the same dimension. Finally, it is not difficult to manipulate Eq. (4.6) to the following more symmetrical form,

$$\det \left| [S_{\approx b}^{-1} + (1 - P_{\approx 1})^{1/2}] \cdot P_{\approx 1}^{-1/2} \cdot [S_{\approx a}^{-1} + (1 - P_{\approx 1})^{1/2}] + P_{\approx 1}^{1/2} \right| = 0 \quad (4.7)$$

which shows that wells a and b enter the eigenvalue equation on equal footings. The matrices  $S_{\approx a}$ ,  $S_{\approx b}$ , and  $P_{\approx 1}$  are functions of the total energy E, and the roots of Eq. (4.7) give the (real) eigenvalues of the multidimensional double well potential.

Recent quantum mechanical calculations by Bowman et al.<sup>19</sup> of the splittings in a symmetric double well potential, coupled to one transverse vibrational mode, provide an interesting example with which to test the branching model. For our calculations the SCP-IOS approximation described in Section IIc was used to construct  $S_{\approx a}(E)$ , which is identical to  $S_{\approx b}$  for the case of a symmetric double well, and  $P_{\approx}$ . Table I shows the results obtained from Eq. (4.7) for the splitting of the nearly degenerate doublets, the most sensitive quantity for such systems, compared to Bowman's (correct) quantum results. (Splittings for higher energy levels were not attempted since in this case Bowman's model potential has more than two wells.) One sees here, too, that the overall model--the semiclassical multichannel model plus the SCP-IOS reaction path treatment for the required component parts--provides a good description of the phenomenon.

## V. Reaction Probabilities

Consider now a reactive potential energy surface for which the potential along the reaction coordinate is as sketched in Figure 6. Reaction corresponds to motion from region a ( $s \rightarrow -\infty$ ) to region b ( $s \rightarrow +\infty$ ) and as before, the (F-1) transverse vibrational modes are not indicated in the figure.

One of us earlier proposed a "unified" statistical model<sup>11</sup> to describe the average reaction probability on such potential surfaces for which there are two "bottlenecks" of the motion (in this case the two barriers). The goal was to have a simple model that "unified" transition state theory, which is correct if there is only one significant bottleneck to the reaction, and phase space theory, which is correct if there exist two bottlenecks with a long-lived collision complex between them. The "unified" model does indeed accomplish this, but it incorporates an implicit assumption of microcanonical equilibrium in the region between the two bottlenecks. Here we show how this assumption can be relaxed by using the multichannel branching model.

Here it is convenient to let  $S_{\approx a}$ ,  $S_{\approx 0}$ , and  $S_{\approx b}$  be transition amplitudes for the intervals (see Figure 6)  $(-\infty, s_1)$ ,  $(s_2, s_3)$ , and  $(s_4, +\infty)$ , respectively. (Note that here  $S_{\approx 0}$  is the S-matrix for a single pass across the well, not a complete oscillation in it.)  $S_{\approx a}$ ,  $S_{\approx 0}$ ,  $S_{\approx b}$  are in general rectangular matrices since the numbers of transverse vibrational states that are energetically open at  $s = -\infty, s_1, s_2, s_3, s_4$  and  $+\infty$  are in general different.  $P_{\approx 1}$  and  $P_{\approx 2}$  are, as before, the (diagonal) matrices of tunneling probabilities for barriers 1 and 2. These quantities can all be

approximated, as in the previous applications, via the SCP-IOS reaction path model described in Section IIc. The branching analysis goes very much as in Section II with obvious modifications. The first two "trajectories", for example, that contribute to the  $a \rightarrow b$  reaction correspond to going straight across the inside well, with amplitude

$$S_{\approx b} \cdot P_{\approx 2}^{1/2} \cdot S_{\approx 0} \cdot P_{\approx 1}^{1/2} \cdot S_{\approx a} \quad ,$$

and to making one extra oscillation back and forth across the well, with amplitude

$$- S_{\approx b} \cdot P_{\approx 2}^{1/2} \cdot S_{\approx 0} \cdot (1-P_{\approx 1})^{1/2} \cdot S_{\approx 0}^{tr} \cdot (1-P_{\approx 2})^{1/2} \cdot S_{\approx 0} \cdot P_{\approx 1}^{1/2} \cdot S_{\approx a} \quad ,$$

and so on. (Here  $S_{\approx 0}^{tr}$ , the transpose of  $S_{\approx 0}$ , is the amplitude for going across the well in the negative direction.) It is easy to write down the amplitude for the general such trajectory and to sum over them all, giving the net amplitude for the  $a \rightarrow b$  reaction as

$$S_{\approx b \leftarrow a}(E) = S_{\approx b} \cdot P_{\approx 2}^{1/2} \cdot S_{\approx 0} \cdot [1 + (1-P_{\approx 1})^{1/2} \cdot S_{\approx 0}^{tr} \cdot (1-P_{\approx 2})^{1/2} \cdot S_{\approx 0}]^{-1} \cdot P_{\approx 1}^{1/2} \cdot S_{\approx a} \quad . \quad (5.1)$$

Equation (5.1), of course, describes the  $a \rightarrow b$  reaction at a much greater level of detail than the "unified" statistical model. (It also requires correspondingly more input in order to implement it.) For example, the energy dependence of  $S_{\approx b \leftarrow a}(E)$  will in general show the complicated resonance structure corresponding to the formation and decay of metastable states (i.e., collision complexes) in the inside well region. The energies and lifetimes of these individual metastable

states are given, as in Section III, by the poles of the S-matrix, which from Eq. (5.1) one easily sees are the complex energies E for which

$$\det \left| 1 + (1-P_1)^{1/2} \cdot S_{\approx 0}^{\text{tr}} \cdot (1-P_2)^{1/2} \cdot S_{\approx 0} \right| = 0 . \quad (5.2)$$

For example, if one turns off the tunneling, i.e., sets  $P_1 = P_2 = 0$ , then this equation reads

$$\det \left| 1 + S \right| = 0 ,$$

where here  $S \equiv S_{\approx 0}^{\text{tr}} \cdot S_{\approx 0}$  is the S-matrix for one complete oscillation in the well; this is the same eigenvalue equation for a single well obtained earlier, Eq. (2.8).

In many cases, though, one may be interested only in an energy-averaged reaction probability and not in the level of detail provided by Eq. (5.1). This is equivalent to neglecting all the cross terms in constructing the reaction probabilities

$$(P_{\approx b, a})_{\approx n, \approx n'} \equiv |(S_{\approx b, a})_{\approx n, \approx n'}|^2 . \quad (53)$$

The branching model for this average reaction probability thus becomes

$$\begin{aligned} P_{\approx b \leftarrow a} &= P_{\approx b} \cdot P_{\approx 2} \cdot P_{\approx 0} \cdot P_{\approx 1} \cdot P_{\approx a} \\ &+ P_{\approx b} \cdot P_{\approx 2} \cdot P_{\approx 0} \cdot (1-P_{\approx 1}) \cdot P_{\approx 0}^{\text{tr}} \cdot (1-P_{\approx 2}) \cdot P_{\approx 0} \cdot P_{\approx 1} \cdot P_{\approx a} \\ &+ \dots , \end{aligned} \quad (54)$$

where the rectangular matrices  $P_{\approx a}$ ,  $P_{\approx 0}$  and  $P_{\approx b}$  are defined by

$$(P)_{\approx a, n, n'} = |(S)_{\approx a, n, n'}|^2$$

etc. Equation (5.2) is a geometric series that is easily summed to give

$$P_{\approx b \leftarrow a} = P_{\approx b} \cdot P_{\approx 2} \cdot P_{\approx 0} \cdot [1 - (1 - P_{\approx 1}) \cdot P_{\approx 0}^{\text{tr}} \cdot (1 - P_{\approx 2}) \cdot P_{\approx 0}]^{-1} \cdot P_{\approx 1} \cdot P_{\approx a} \quad (5.5)$$

We note that Eq. (5.4), which is the result of a classical multichannel branching model, has no resonance structure in its energy dependence, for this is all lost when the interference between the different "trajectories" that contribute to the  $a \rightarrow b$  reaction is neglected.

The reaction probability of Eq. (5.4), although less detailed than that given by Eq. (5.2), still has more information than the "unified" statistical model.

## VI. Concluding Remarks

Our goal in developing the semiclassical branching model described above is to have a simple but reasonably quantitative methodology for utilizing ab initio quantum chemical reaction path calculations to describe various aspects of polyatomic reaction dynamics. Such ab initio quantum chemical calculations provide the quantities  $[V_0(s), \{\omega_k(s)\}, \text{ and } \{B_{k,k}(s)\}]$  which characterize the reaction path Hamiltonian, and then the SCP-IOS approximation provides the "components" that go into the formulae obtained from the branching model. One thus has a complete machinery for an ab initio polyatomic reaction dynamics. The numerical examples presented above indicate the overall approach to be quantitatively accurate enough to be of considerable use when applied to real polyatomic systems.

In concluding we note that although the presentation in Section II, for example, assumed that the potential along the reaction path,  $V_0(s)$ , has an actual barrier (cf. Figure 1), it is actually not necessary that this be the case. Suppose, for example, that  $V_0(s)$  is a Morse potential

$$V_0(s) = D[e^{-2\alpha(s-s_0)} - 2e^{-\alpha(s-s_0)}] \quad (6.1)$$

For energy  $E$  the classical turning points, defined by  $V_0(s) = E$ , are

$$s = s_0 - \frac{1}{\alpha} \ln(1 \pm \sqrt{1 + E/D}) \quad (6.2)$$

For  $E < 0$  there are two real turning points, as expected, while for  $E > 0$  the "+" sign in Eq. (6.2) gives the real inner turning point,



$$s_1 = s_0 - \frac{1}{\alpha} \ln(1 + \sqrt{1+E/D}) \quad , \quad (6.3)$$

and the "-" sign gives a complex outer turning point

$$\begin{aligned} s_2 &= s_0 - \frac{1}{\alpha} \ln(1 - \sqrt{1+E/D}) \\ &= s_0 - \frac{1}{\alpha} \ln(\sqrt{1+E/D} - 1) \pm i \frac{\pi}{\alpha} \quad . \quad (6.4) \end{aligned}$$

The action integral  $\theta$  between these two complex outer turning points is negative, so that the situation is entirely equivalent to the "over barrier" case. Thus Eq. (2.17) provides the transmission probability of passing into or out of the well from the outside (even though for real  $s$  there is no physical barrier that identifies the "inside" and "outside".) As noted in Section III, results obtained in over barrier cases were essentially as good as in the under barrier (i.e., tunneling) cases, so it seems clear that the model should apply equally well even if there is no (real) barrier.

Appendix A: Real Eigenvalues in the Perturbative Limit

Here we consider Eq. (2.8),

$$\det | \underset{\sim}{1} + \underset{\sim}{S}(E) | = 0 \quad , \quad (A.1)$$

the equation which determines real eigenvalues in a multidimensional potential well.  $\underset{\sim}{S}(E)$  (here the "o" has for convenience been dropped) is the S-matrix per oscillation in the effective potential well  $V_a(s)$ . The goal here is to show that in the perturbative limit Eq. (A.1) gives essentially the same results as ordinary quantum mechanical perturbation theory for eigenvalues. Thus the off-diagonal elements of  $\underset{\sim}{S}$  are assumed to be small, and the diagonal elements are those of the unperturbed system,

$$\underset{\sim}{S}_{\underset{\sim}{n},\underset{\sim}{n}}(E) = e^{2i\eta(\underset{\sim}{n},E)} \quad , \quad (A.2)$$

where  $\eta$  is the phase shift for one pass across the well for channel  $\underset{\sim}{n}$ .

To make a perturbative expansion of Eq. (A.1) we use the following general relation that is easy to derive: The determinant of any matrix  $\underset{\sim}{A}$  is given to lowest order in its off-diagonal elements by

$$\det | \underset{\sim}{A} | = \det | \underset{\sim}{A}_0 | \times \left[ 1 - \frac{1}{2} \sum_{\substack{k,k' \\ k \neq k'}} \frac{A_{kk'} A_{k'k}}{A_{kk} A_{k'k'}} \right] \quad (A.3)$$

where  $\underset{\sim}{A}_0$  is the diagonal part of  $\underset{\sim}{A}$ . Applied to Eq. (A.1), Eq. (A.3) gives

$$0 = \det |1 + S_{\approx 0}(E)| \times [1 - \frac{1}{2} \sum_{\substack{\tilde{n}, \tilde{n}' \\ \tilde{n} \neq \tilde{n}'}} \frac{S_{\tilde{n}, \tilde{n}'} S_{\tilde{n}', \tilde{n}}}{(1 + e^{2i\eta(\tilde{n}, E)})(1 + e^{2i\eta(\tilde{n}', E)})}] \quad (\text{A.4})$$

where  $S_{\approx 0}$  is the diagonal part of  $S$ . Since  $\det |1 + S_{\approx 0}(E)| \neq 0$ --for this factor is zero only for E equal to a zero<sup>th</sup> order energy level-- Eq. (A.4) implies that

$$1 = \frac{1}{2} \sum_{\substack{\tilde{n}, \tilde{n}' \\ \tilde{n} \neq \tilde{n}'}} \frac{S_{\tilde{n}, \tilde{n}'}^2}{[1 + e^{2i\eta(\tilde{n}, E)}][1 + e^{2i\eta(\tilde{n}', E)}]} \quad , \quad (\text{A.5})$$

where the symmetry of the S-matrix has been utilized.

To proceed further we note that the zero<sup>th</sup> order energy levels  $\{E_{\tilde{n}, n_s}^0\}$ , where  $n_s$  is the quantum number for the s-degree of freedom, are defined semiclassically by

$$\eta(\tilde{n}, E) = (n_s + \frac{1}{2})\pi \quad , \quad (\text{A.6})$$

which shows that the factor  $(1 + e^{2i\eta(\tilde{n}, E)})^{-1}$  in Eq. (A.5) has a polar singularity when E is equal to one of the zero<sup>th</sup> order energy levels with the same value of the transverse quantum numbers. More specifically, for E close to the particular zero<sup>th</sup> order eigenvalue  $E_{\tilde{n}, n_s}^0$ , a Taylors series expansion gives

$$(1 + e^{2i\eta(\tilde{n}, E)})^{-1} \approx [(E - E_{\tilde{n}, n_s}^0)(-2i) \frac{\partial \eta(\tilde{n}, E_{\tilde{n}, n_s}^0)}{\partial E}]^{-1} \quad .$$

Since this polar structure is true for all values of the quantum number  $n_s$ , the complete energy dependence of this factor can be reasonably well represented by a sum of such pole terms; i.e., one has

$$[1 + e^{2i\eta(\tilde{n}, E)}]^{-1} \approx \sum_{\tilde{n}_s} (E - E_{\tilde{n}, \tilde{n}_s}^0)^{-1} \frac{\partial E_{\tilde{n}, \tilde{n}_s}^0}{\partial \tilde{n}_s} / (-2\pi i) \quad , \quad (A.7)$$

where we have utilized the fact that

$$\left. \frac{\partial \eta(\tilde{n}, E)}{\partial E} \right|_{E=E_{\tilde{n}, \tilde{n}_s}^0} = \pi / \frac{\partial E_{\tilde{n}, \tilde{n}_s}^0}{\partial \tilde{n}_s} \quad . \quad (A.8)$$

With Eq. (A.7), the eigenvalue equation, (A.5), reads

$$1 = \frac{1}{2} \sum_{\substack{\tilde{n}''', \tilde{n}' \\ \tilde{n}'' \neq \tilde{n}'}} \sum_{\tilde{n}_s''', \tilde{n}_s'} (E - E_{\tilde{n}''', \tilde{n}_s'''}^0)^{-1} (E - E_{\tilde{n}', \tilde{n}_s'}^0)^{-1} S_{\tilde{n}'', \tilde{n}'}(E)^2 \\ \frac{\partial E_{\tilde{n}''', \tilde{n}_s'''}^0}{\partial \tilde{n}_s'''} \frac{\partial E_{\tilde{n}', \tilde{n}_s'}^0}{\partial \tilde{n}_s'} / (-2\pi i)^2 \quad . \quad (A.9)$$

We now look for a root of Eq. (A.9) that is close to a particular zero<sup>th</sup> order energy level,  $E_{\tilde{n}, \tilde{n}_s}^0$ , say; i.e., we set

$$E = E_{\tilde{n}, \tilde{n}_s}^0 + \Delta E_{\tilde{n}, \tilde{n}_s} \quad ,$$

where  $\Delta E_{\tilde{n}, \tilde{n}_s}$  is small. When this is substituted into Eq. (A.9) the dominant terms are those for which either  $(\tilde{n}', \tilde{n}_s')$  or  $(\tilde{n}'', \tilde{n}_s'')$  equal  $(\tilde{n}, \tilde{n}_s)$  and Eq. (A.9) thus becomes

$$1 = \frac{1}{\Delta E_{\tilde{n}, \tilde{n}_s}} \sum_{\tilde{n}', \tilde{n}_s'} (E_{\tilde{n}, \tilde{n}_s}^0 - E_{\tilde{n}', \tilde{n}_s'}^0)^{-1} S_{\tilde{n}, \tilde{n}'}^2 \frac{\partial E_{\tilde{n}, \tilde{n}_s}^0}{\partial \tilde{n}_s} \frac{\partial E_{\tilde{n}', \tilde{n}_s'}^0}{\partial \tilde{n}_s'} / (-2\pi i)^2 \quad (A.10)$$

which gives the standard quantum mechanical second order perturbation expression

$$\Delta E_{\tilde{n}, \tilde{n}_s} = \sum_{\substack{\tilde{n}' \tilde{n}'_s \\ \tilde{n} \tilde{n}_s}} \frac{H_{\tilde{n}\tilde{n}_s, \tilde{n}'\tilde{n}'_s}^2}{E_{\tilde{n}\tilde{n}_s}^0 - E_{\tilde{n}'\tilde{n}'_s}^0}, \quad (A.11)$$

provided we establish the following correspondence:

$$H_{\tilde{n}\tilde{n}_s, \tilde{n}'\tilde{n}'_s} \leftrightarrow S_{\tilde{n}, \tilde{n}'}(\bar{E}) \sqrt{\frac{\partial E_{\tilde{n}\tilde{n}_s}^0}{\partial \tilde{n}_s} \frac{\partial E_{\tilde{n}'\tilde{n}'_s}^0}{\partial \tilde{n}'_s}} / (-2\pi i) \quad (A.12)$$

Equation (A.12) can be established by noting the perturbative approximation for the S-matrix element in the classical path limit:

$$S_{\tilde{n}, \tilde{n}'}(\bar{E}) = -i \int ds e^{i[\delta_{\tilde{n}}(s) - \delta_{\tilde{n}'}(s)]} H_{\tilde{n}\tilde{n}'}(s)/v(s), \quad (A.13)$$

where the integral is over one oscillation in the s-well and  $v(s) = \sqrt{2[E - V_a(s)]}$  is the local velocity (i.e.,  $\int ds/v(s) = \int dt$ , where t is the time). Since

$$\frac{\partial E_{\tilde{n}, \tilde{n}_s}}{\partial \tilde{n}_s} = \frac{2\pi}{\tau_{\tilde{n}_s}}, \quad (A.14)$$

where  $\tau_{\tilde{n}_s}$  is the period of the s-oscillation, Eq. (A.12) thus reads

$$H_{\tilde{n}\tilde{n}_s, \tilde{n}'\tilde{n}'_s} \leftrightarrow \frac{1}{\tau_{\tilde{n}_s}} \int \frac{ds}{v(s)} e^{i[\delta_{\tilde{n}}(s) - \delta_{\tilde{n}'}(s)]} H_{\tilde{n}, \tilde{n}'}(s) \quad (A.15)$$

When one realizes that the phase factor in the integrand of Eq. (A.15) is the adiabatic version of  $\exp[i(E_{\tilde{n},\tilde{n}_s}^0 - E_{\tilde{n}',\tilde{n}'_s})t/\hbar]$ , the RHS of Eq. (A.15) is recognized as the usual<sup>20</sup> semiclassical approximation to the matrix element on the LHS.

This analysis thus shows that, in the perturbative limit at least, the multichannel aspect of the eigenvalue equation given by the branching model, Eq. (A.1), does indeed correspond to the correct quantum mechanical perturbation expression for eigenvalues.

Appendix B: Feshbach Resonances in the Perturbative Limit

A slight modification of the perturbative analysis in Appendix A can be used to show that the multichannel branching model is also capable of describing Feshbach resonances,<sup>15</sup> i.e., metastable states that are more naturally thought of as being formed by temporary excitation of (asymptotically) closed channels rather than by being trapped by a barrier as in Figure 1.

Suppose, therefore, that the effective potential along the reaction coordinate in Figure 1 is replaced by a Morse-like potential, i.e., one for which there is no actual barrier. As noted in Section VI, however, there still exists an "effective barrier" in the sense that there is a complex turning point and a non-unit probability of making a transition from the "outside" to the "inside" region of the potential well. The situation is entirely equivalent to there being an actual barrier with the energy above it. The real part of the complex turning point effectively defines the division between the "inside" and the "outside" regions of the potential.

The complex eigenvalues of the system are thus still given within the branching model by Eq. (2.5),

$$\det \left| 1 + (1-P)^{1/2} \cdot S \right| = 0 \quad , \quad (B.1)$$

where  $S \equiv S(E)$  (the subscript "0" has for convenience been dropped) is the S-matrix per oscillation in the "inside" region of the potential well (determined by the real inner turning point and the complex outer turning point). If one now considers the perturbative limit, as in

Appendix A, then Eq. (B.1) leads in a similar fashion to the obvious generalization of Eq. (A.5):

$$1 = \frac{1}{2} \sum_{\substack{\underline{n}, \underline{n}' \\ \underline{n} \neq \underline{n}'}} \frac{(1-P_{\underline{n}})^{1/2} S_{\underline{n}, \underline{n}'} (1-P_{\underline{n}'})^{1/2} S_{\underline{n}', \underline{n}}}{[1+(1-P_{\underline{n}})^{1/2} e^{2i\eta(\underline{n}, E)}][1+(1-P_{\underline{n}'})^{1/2} e^{2i\eta(\underline{n}', E)}]} \quad (\text{B.2})$$

For open channels, i.e., values of  $\underline{n}$  for which  $E > V_0(s) + \hbar\omega \cdot (\underline{n} + \frac{1}{2})$  as  $s \rightarrow +\infty$ , the transmission probability  $P_{\underline{n}}$  is given by Eq. (2.17), where  $\theta$  is negative for this "over barrier" situation, so that one has

$$(1-P_{\underline{n}})^{1/2} \approx e^{-|\theta(\underline{n})|}$$

For closed channels, on the other hand, i.e., those for which  $E < V_0(s) + \hbar\omega \cdot (\underline{n} + \frac{1}{2})$  as  $s \rightarrow +\infty$ , it is clear that one must have  $P_{\underline{n}} = 0$ . Equation (B.2) thus specializes to the following:

$$\begin{aligned} 1 = & \frac{1}{2} \sum_{\underline{n}}^{\text{C}} \sum_{\underline{n}'}^{\text{C}} \frac{S_{\underline{n}, \underline{n}'}^2}{[1+e^{2i\eta(\underline{n}, E)}][1+e^{2i\eta(\underline{n}', E)}]} \\ & + \sum_{\underline{n}}^{\text{C}} \sum_{\underline{n}'}^{\text{O}} \frac{S_{\underline{n}, \underline{n}'}^2 e^{-|\theta(\underline{n}')|}}{[1+e^{2i\eta(\underline{n}, E)}]} \\ & + \frac{1}{2} \sum_{\underline{n}}^{\text{O}} \sum_{\underline{n}'}^{\text{O}} S_{\underline{n}, \underline{n}'}^2 e^{-|\theta(\underline{n})|} e^{-|\theta(\underline{n}')|} \quad , \quad (\text{B.3}) \end{aligned}$$

where the subscript "O" or "C" on the summation symbol indicates a sum over the open or closed channels, respectively. Since one typically



expects  $\exp[-|\theta(\tilde{n})|] \ll 1$ , the approximation

$$1 + e^{-|\theta(\tilde{n})|} e^{2i\eta(\tilde{n}, E)} \approx 1$$

has also been incorporated in Eq. (B.3).

One notes that the first term on the RHS of Eq. (B.3), that involving only the closed channels, is identical to Eq. (A.5) of Appendix A. Therefore if only this term were retained in Eq. (B.3), the equation would determine real eigenvalues and the system would thus be stable. (In the usual notation of Feshbach analysis<sup>15</sup> these would be the branching model's approximation to the eigenvalues of  $H_{QQ}$ , the closed channel Hamiltonian.) As we shall see presently, it is the second term in Eq. (B.3), the one which couples open and closed channels, that gives rise to an imaginary part to the eigenvalue and thus causes the system to be metastable. (The third term, that involving open channel--open channel couples is smaller still and will be neglected for the present discussion.)

Proceeding as in Appendix A, the energy  $E$  is assumed to be close to a particular (real) zero<sup>th</sup> order closed channel eigenvalue,

$$E = E_{\tilde{n}, n_s}^{(0)} + \Delta E_{\tilde{n}, n_s},$$

where  $\Delta E_{\tilde{n}, n_s}$  is small and  $\tilde{n}$  is a closed channel. Utilizing Eq. (A.7) and continuing as before, Eq. (B.3) then gives  $\Delta E_{\tilde{n}, n_s}$  as

$$\begin{aligned}
 \Delta E_{\tilde{n}, n_s} = & \sum_{\tilde{n}'} C \sum_{\tilde{n}_s'} (E_{\tilde{n}, n_s}^{(0)} - E_{\tilde{n}', n_s'}^{(0)})^{-1} \frac{\partial E_{\tilde{n}, n_s}}{\partial n_s} \frac{\partial E_{\tilde{n}', n_s'}}{\partial n_s'} \\
 & \times [S_{\tilde{n}, \tilde{n}'} / (-2\pi i)]^2 \\
 & + \sum_{\tilde{n}'}^0 e^{-|\theta(\tilde{n}')|} \frac{\partial E_{\tilde{n}, n_s}^{(0)}}{\partial n_s} S_{\tilde{n}, \tilde{n}'}^2 / (-2\pi i) \quad . \quad (B.4)
 \end{aligned}$$

The first term in Eq. (B.4), which describes the effect of other closed channels on the closed channel eigenvalue  $E_{\tilde{n}, n_s}^{(0)}$ , is of the same form as that obtained in Appendix A; it is a real second-order perturbation correction to the energy of the metastable state. Since  $S_{\tilde{n}, \tilde{n}'}^2 < 0$ , one sees that the second term of Eq. (B.4), which describes the effect of open channels on the closed channel eigenvalue, is negative imaginary and thus gives a perturbative approximation to the width of the metastable state. One also sees that the width implied by Eq. (B.4) has the same form as that given by Feshbach theory<sup>15</sup> in its lowest order perturbative limit, i.e.,

$$\Gamma_{\tilde{n}, n_s} \approx \sum_{\tilde{n}'}^0 2\pi\rho |H_{\tilde{n}, \tilde{n}'}|^2 \quad ,$$

where  $\rho$  is a normalization factor.

One thus sees that the semiclassical multichannel branching model is capable, in principle at least, of describing Feshbach-type metastable states as well as those caused by tunneling through a barrier.

Acknowledgments

This work has been supported by the Director, Office of Energy Research, Office of Basic Energy Sciences, Chemical Sciences Division of the U.S. Department of Energy under Contract Number W-7405-ENG-48. All calculations were carried out on a Harris H800, funded by National Science Foundation Grant CHE-79-20181. WHM also acknowledges the kind hospitality of the Lehrstuhl für Theoretische Chemie, Technische Universität München and a U.S. Senior Scientist Humboldt Award.

References

1. B. A. Waite and W. H. Miller, (a) J. Chem. Phys. 73, 3713 (1980);  
(b) J. Chem. Phys. 74, 3910 (1981).
2. Some recent experimental results related to this question are  
(a) K. V. Reddy and M. V. Berry, Chem. Phys. Lett. 66, 223 (1979);  
(b) R. Naaman, D. M. Lubman, and R. N. Zare, J. Chem. Phys. 71, 4192  
(1979); (c) R. B. Hall and A. Kaldor, J. Chem. Phys. 70, 4027 (1979);  
(d) Advances in Laser Chemistry, edited by A. H. Zewail (Springer,  
New York, 1978); (e) Laser-Induced Processes in Molecules, edited  
by K. L. Kompa and S. D. Smith (Springer, New York, 1979); (f)  
B. D. Cannon and F. F. Crim, J. Chem. Phys. 75, 1752 (1981).
3. The earliest such calculations of this type were by D. L. Bunker and  
his associates. For a recent review, see W. L. Hase in Dynamics of  
Molecular Collisions Part B, Vol. 2 of Modern Theoretical Chemistry,  
edited by W. H. Miller (Plenum, New York, 1976).
4. W. H. Miller, J. Am. Chem. Soc. 101, 6810 (1979); S. K. Gray, W. H.  
Miller, Y. Yamaguchi, and H. F. Schaefer, J. Am. Chem. Soc. 103, 1900  
(1981).
5. R. J. Wolf and W. L. Hase, J. Chem. Phys. 73, 3779 (1980).
6. E. J. Heller and M. J. Davis, J. Phys. Chem. 85, 307 (1981).
7. W. H. Miller, (a) Adv. Chem. Phys. 25, 69 (1974); (b) Adv. Chem.  
Phys. 30, 77 (1975).
8. For other applications of the one-dimensional branching model, see  
W. H. Miller, J. Phys. Chem. 83, 960 (1979).
9. W. H. Miller, N. C. Handy, and J. E. Adams, J. Chem. Phys. 72, 99  
(1980).
10. W. H. Miller and S.-h. Shi, J. Chem. Phys. 75, 2258 (1981).

11. W. H. Miller, J. Chem. Phys. 65, 2216 (1976). See also W. H. Miller in Potential Energy Surfaces and Dynamics Calculations (ACS Symp. Series), edited by D. G. Truhlar (Plenum, N.Y., 1981), p. 265.
12. R. P. Feynman and A. R. Hibbs, Quantum Mechanics and Path Integrals (McGraw Hill, New York, 1965).
13. See, for example, T.-Y. Wu and T. Ohmura, Quantum Theory of Scattering (Prentice-Hall, Englewood Cliffs, 1962).
14. See, for example, W. H. Miller, J. Chem. Phys. 48, 1651 (1968).
15. H. Feshbach, Ann. Phys. (N.Y.) 5, 357 (1958); 19, 287 (1962).
16. S. K. Gray, W. H. Miller, Y. Yamaguchi, and H. F. Schaefer, J. Chem. Phys. 73, 2733 (1980).
17. C. J. Cerjan, S.-h. Shi, and W. H. Miller, J. Phys. Chem. (1981).
18. See, for example, D. G. Truhlar and A. Kuppermann, J. Chem. Phys. 56, 2232 (1972).
19. K. M. Christoffel and J. M. Bowman, J. Chem. Phys. 74, 5057 (1981).
20. See, for example, L. D. Landau and E. M. Lifshitz, Quantum Mechanics (Pergamon, New York, 1958), p. 178-183.

Table I. Energy Level Splittings in a Two-Dimensional Symmetric Double Well Potential.

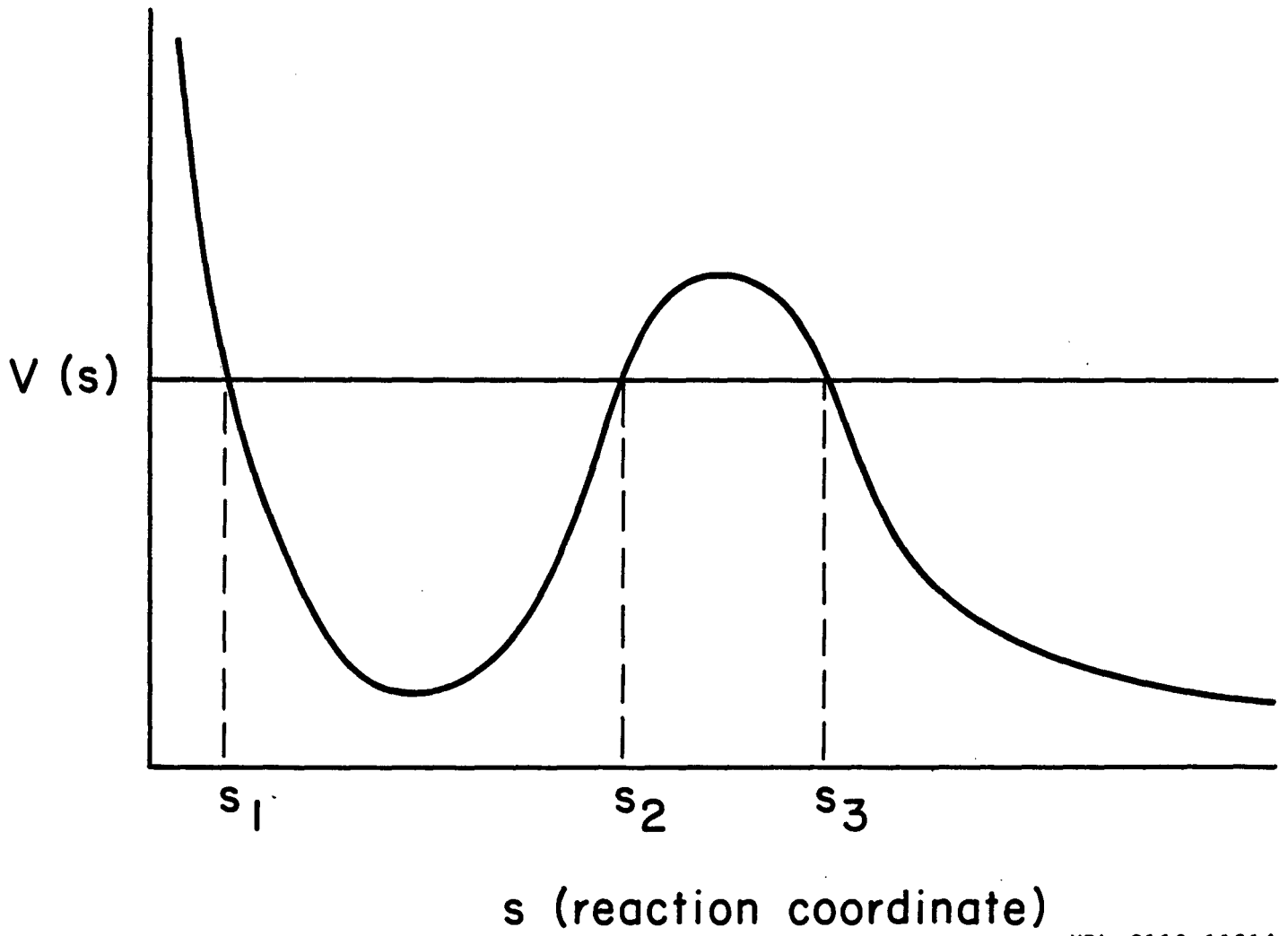
		<u>Splittings (cm<sup>-1</sup>)</u>		
		<u>Transverse Quantum No. (n<sub>y</sub>)</u>	<u>Branching Model Results<sup>a</sup></u>	<u>Exact Quantum Results<sup>b</sup></u>
Lowest Doublet		0	0.91	0.95
		1	1.23	1.28
		2	1.68	1.77
<hr style="border-top: 1px dashed black;"/>				
First Excited Doublet		0	47.2	44.4

<sup>a</sup>Present results (see Section IV).

<sup>b</sup>From reference 19.

Figure Captions

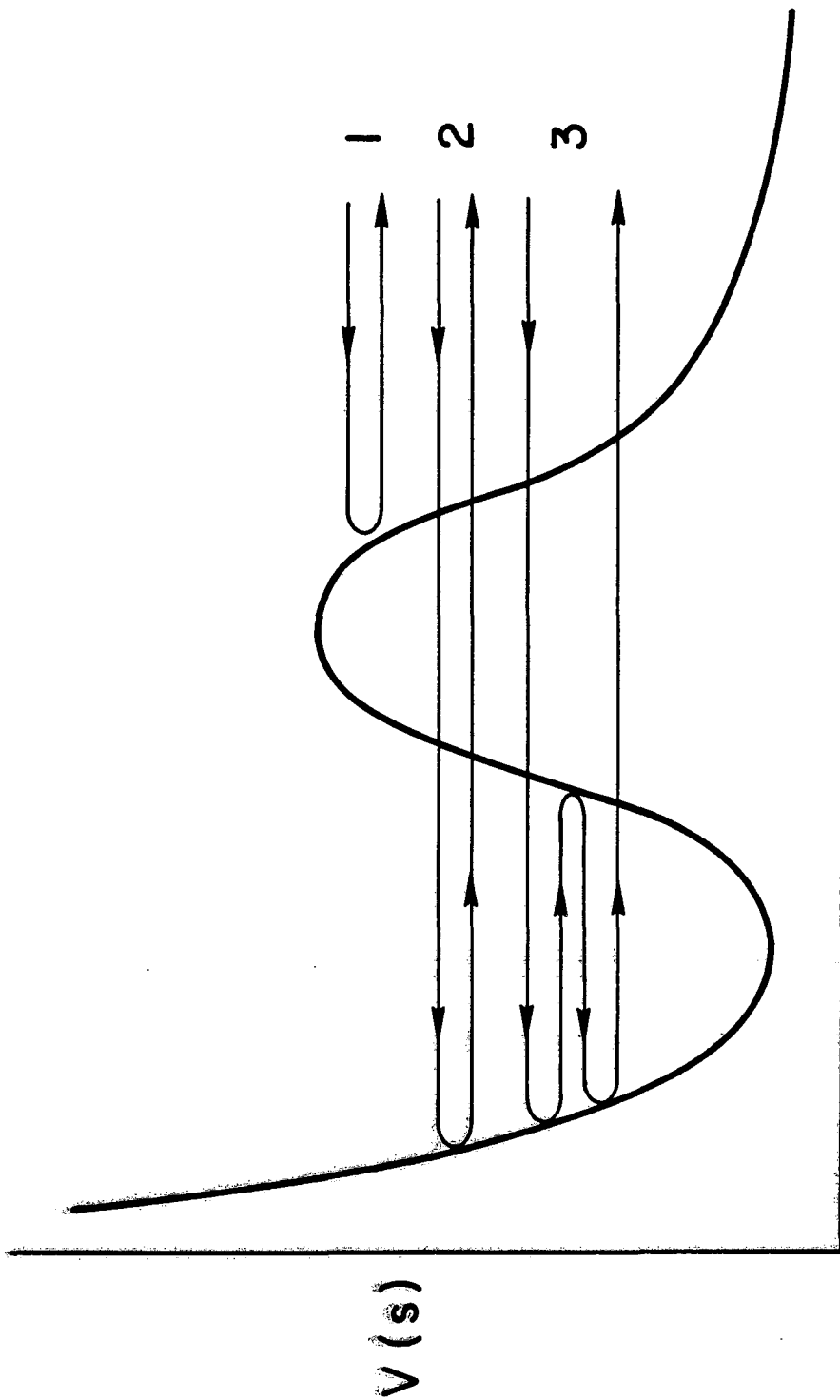
1. Sketch of the effective potential  $V$  along the (mass-weighted) reaction coordinate  $s$  for the situation discussed in Section II.
2. Depiction of the first three "trajectories" of the branching model, the amplitudes associated with which are given by Eqs. (2.2a), (2.2b), and (2.2c), respectively.
3. Unimolecular decay rates as a function of energy, as given by the branching model, for the individual metastable states of the system described in Section III. The solid points and open points correspond, respectively, to the states that are even and odd with regard to reflection across the  $x$ -axis.
4. Same as Figure 3, except the values shown are from the rigorous quantum calculations of reference 1b.
5. Sketch of the effective potential  $V$  along the (mass-weighted) reaction coordinate  $s$ , for the situation discussed in Section IV.
6. Same as Figure 5, except for the situation discussed in Section V.



XBL 8110-11914

Figure 1





$s$  (reaction coordinate)

XBL 8110-11919

Figure 2

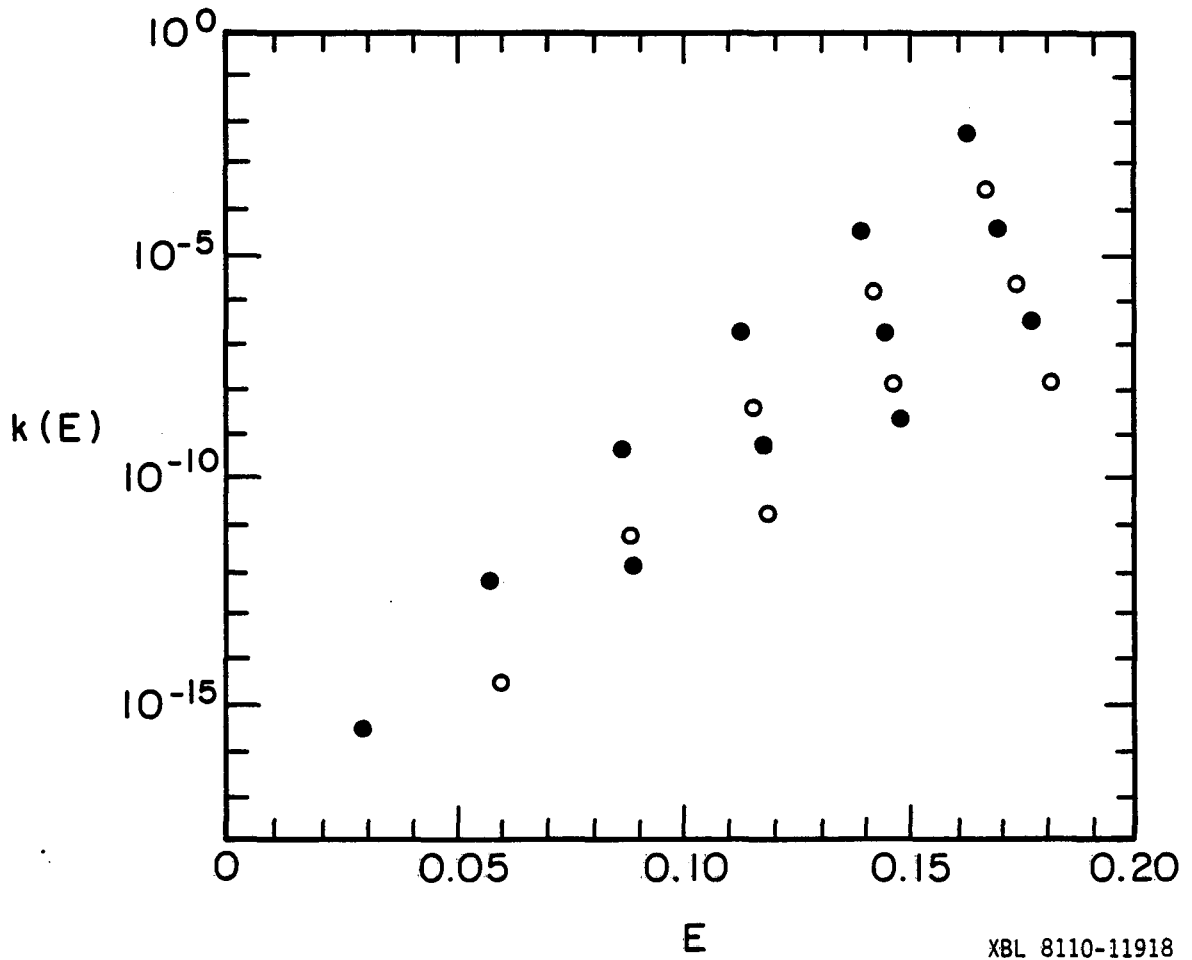


Figure 3

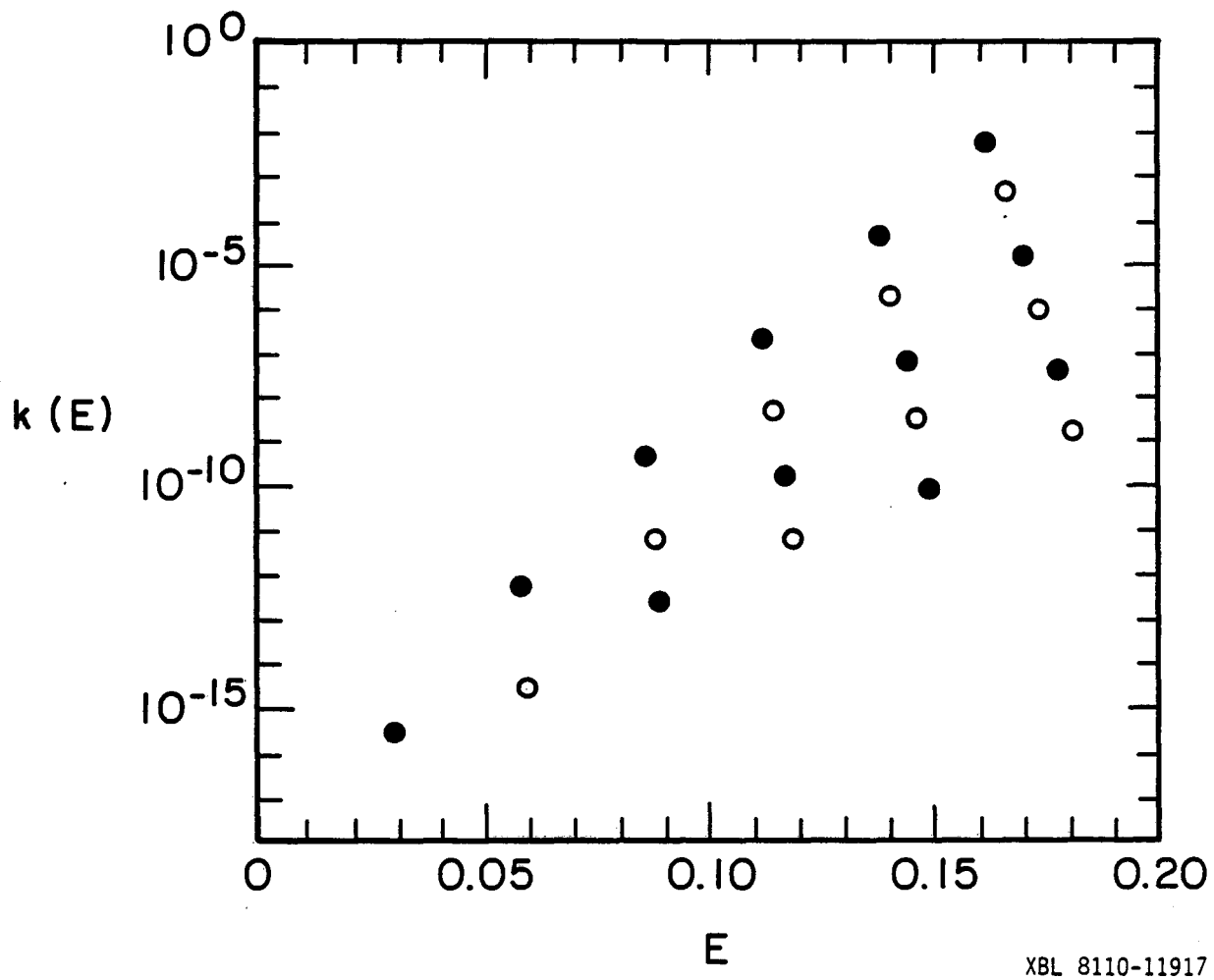
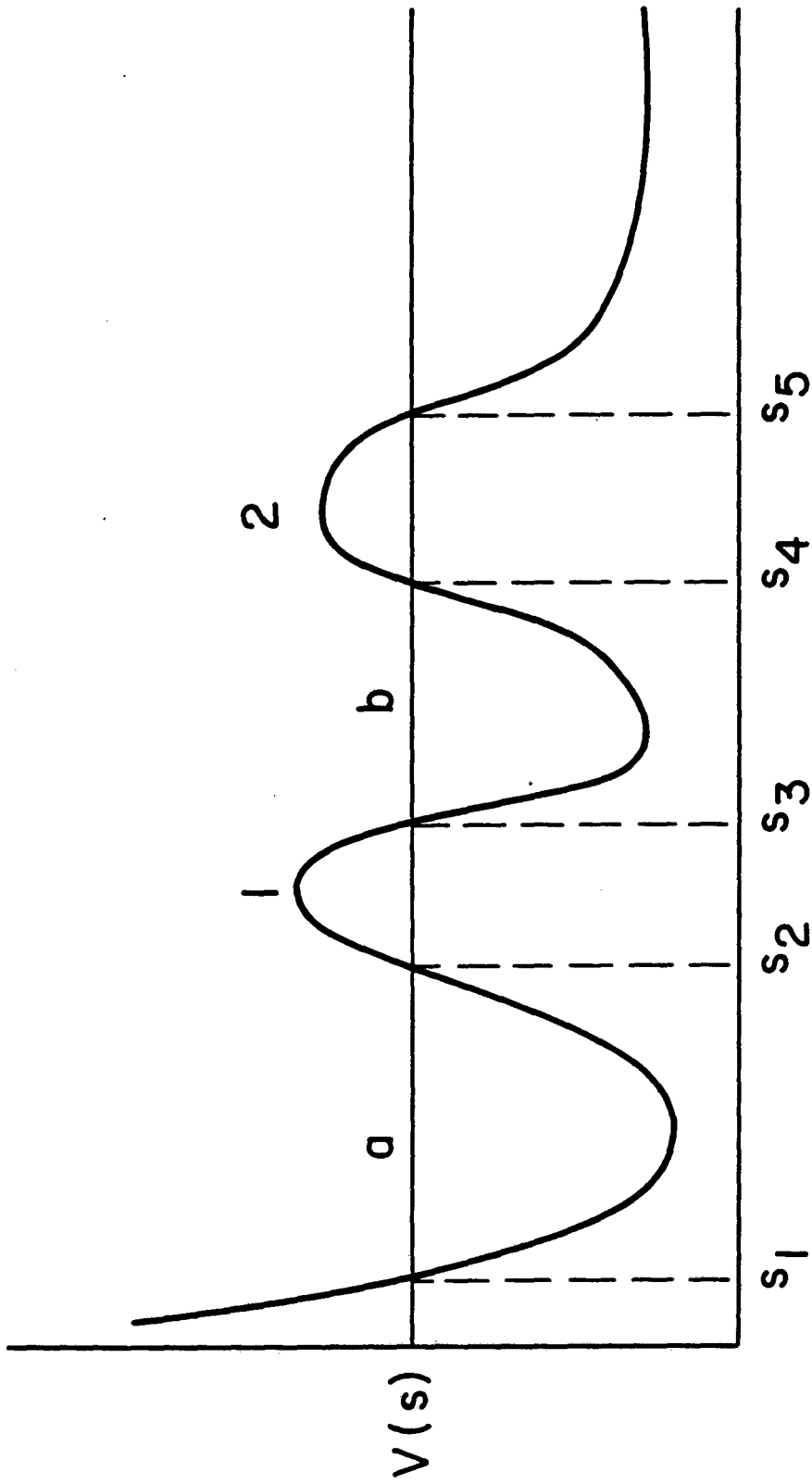


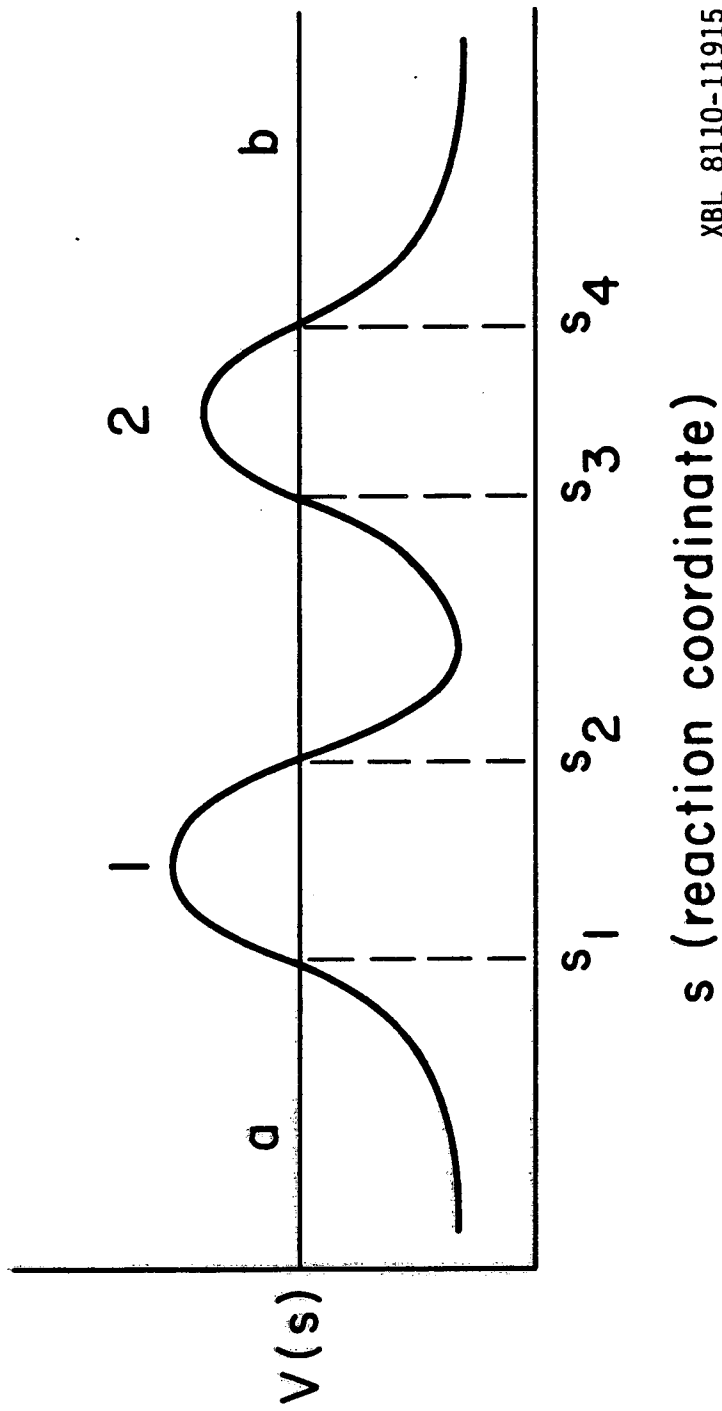
Figure 4



s (reaction coordinate)

XBL 8110-11916

Figure 5



XBL 8110-11915

Figure 6

This report was done with support from the Department of Energy. Any conclusions or opinions expressed in this report represent solely those of the author(s) and not necessarily those of The Regents of the University of California, the Lawrence Berkeley Laboratory or the Department of Energy.

Reference to a company or product name does not imply approval or recommendation of the product by the University of California or the U.S. Department of Energy to the exclusion of others that may be suitable.

TECHNICAL INFORMATION DEPARTMENT  
LAWRENCE BERKELEY LABORATORY  
UNIVERSITY OF CALIFORNIA  
BERKELEY, CALIFORNIA 94720